

https://doi.org/10.1070/QEL16722

Nanosecond room-temperature Fe:ZnSe laser pumped inside the resonator of a transversely diode-pumped Er:YLF laser

V.I. Kozlovsky, Yu.V. Korostelin, Ya.K. Skasyrsky, M.P. Frolov

Abstract. **Lasing at room temperature is obtained in a Fe:ZnSe crystal installed as a passive *Q*-switch in a diode-pumped Er:YLF laser resonator. A miniresonator of the Fe:ZnSe laser is formed by mirrors pressed against the optical surfaces of the crystal with high reflectivities at λ = 4–4.5 μm and a high transmittance for the Er:YLF laser generation lines. In the Er:YLF laser resonator, short pulses of ~100 ns duration at λ = 2.65 μm are generated, stipulated by passive *Q*-switching of the resonator by the Fe:ZnSe crystal. The absorption of the Er:YLF laser radiation in the Fe:ZnSe crystal leads to the pumping of Fe:ZnSe laser, which generates pulses with a duration of less than 50 ns and an energy of ~0.5 μJ at λ = 4.2 μm. The laser operates in the pulse-periodic pump regime with a repetition rate up to 200 Hz.**

Keywords: *mid-IR range, II–VI crystals, Fe:ZnSe laser, Er:YLF laser, passive Q-switching, intracavity pumping.*

1. Introduction

A laser based on a ZnSe crystal doped with divalent Fe ions is one of the most promising lasers for the mid-IR spectral range (4–5 μm) [1–3], which has the atmospheric transparency window. The best energy characteristics of this laser are attained by cooling the crystal with liquid nitrogen [4, 5]. This is explained by the fact that the internal quantum efficiency of the laser transition decreases with increasing temperature due to the activation of multiphonon nonradiative recombination. Recently, a high pulse energy of 7.5 J was attained by cooling the crystal to 220 K using thermoelectric elements [6]. The generation threshold of the Fe:ZnSe laser at room temperature is quite high, and to obtain high efficiency of the laser, it is necessary to use high-power nanosecond pulses with λ = 2.5–3 μm as pump pulses. However, the generation of such pump pulses involves a number of difficulties. In [7, 8], the HF-laser with a pulse duration of ~100 ns was used as a pump source. These lasers are inconvenient for practical use because of the toxicity of the medium used and the cumbersome structure of the device. Another source of pumping is a pulsed Er:YAG laser with a *Q*-switched resonator [9]. These lasers are still operating under lamp pumping. Though short pulses were also obtained in pumping by laser diodes [10], the pulse energy attained is too small for effective pumping of the Fe:ZnSe laser at room temperature. Recently, lower-threshold Er:YLF crystals have been used as active media in diode-pumped lasers [11, 12]. With passive *Q*-switching of such lasers, nanosecond pulses with an energy of 3 mJ, though with a low efficiency, were obtained [13].

In the present work, the generation of nanosecond pulses in a Fe:ZnSe laser at room temperature and relatively low-power laser diode pumping is implemented using a new pump scheme for this type of laser. A miniresonator with a Fe:ZnSe crystal was placed inside the Er:YLF laser resonator with transverse pumping by a laser diode array. In this scheme, the Fe:ZnSe crystal serves as a passive *Q*-switch for the Er:YLF laser and at the same time represents an active element of the Fe:ZnSe laser. A similar approach was first applied in [14, 15], where a laser on the LiF crystal with F_2^--colour centres was pumped inside a three-mirror resonator of the Nd^{3+} laser. In this case, the F_2^-:LiF crystal was a passive *Q*-switch for the Nd^{3+} laser.

2. Experiment

Figure 1 shows the scheme of the experimental setup. In the experiments, we used two single-crystal Fe:ZnSe plates with a thickness of 1.3 (P1) and 1.7 mm (P2). The plates were cut from two crystals grown from the physical vapour transport method using a seed [16]. The concentrations of Fe ions in the first and second plates were 2.3×10^{17} and 9.5×10^{17} cm^{-3}, respectively. The transmission spectra of the plates are shown in Fig. 2. The plates were polished on both sides; the angle between the polished surfaces did not exceed 30″. The plates were originally used as a passive *Q*-switches for the Er:YLF laser. In this case, mirrors (*8*) and (*10*) (see Fig. 1) were removed.

Mirrors (*8*), (*10*) and (*11*) were 1.8-mm-thick plane-parallel sapphire plates of basic orientation with an interference coating made of alternating Si and SiO_2 layers. In the scheme in Fig. 1, identical mirrors (*8*) and (*10*) were used. The transmission spectra of the mirrors are shown in Fig. 3. The noise in the spectra near λ = 3.1 μm and λ = 4.2 μm is associated with absorption by the vapours of water and CO_2. Mirrors (*8*) and (*10*) were tightly pressed against the crystal (*9*), so that optical contact was achieved between the mirrors and crystal. When the plane wave is incident on the mirrors (*8*) and (*10*) (M1 in Fig. 3) not from the air, but from ZnSe (refractive index 2.4), the reflection coefficient decreases. The calculation showed that in the region λ = 4–4.5 μm the reflection coefficient was 99.36%.

V.I. Kozlovsky P.N. Lebedev Physical Institute, Russian Academy of Sciences, Leninsky prosp. 53, 119991 Moscow, Russia; National Research Nuclear University 'MEPhI', Kashirskoye sh. 31, 115409 Moscow, Russia; e-mail: vikoz@sci.lebedev.ru;
Yu.V. Korostelin, Ya.K. Skasyrsky, M.P. Frolov P.N. Lebedev Physical Institute, Russian Academy of Sciences, Leninsky prosp. 53, 119991 Moscow, Russia

Received 8 May 2018; revision received 24 May 2018
Kvantovaya Elektronika **48** (8) 686–690 (2018)
Translated by M.A. Monastyrskiy

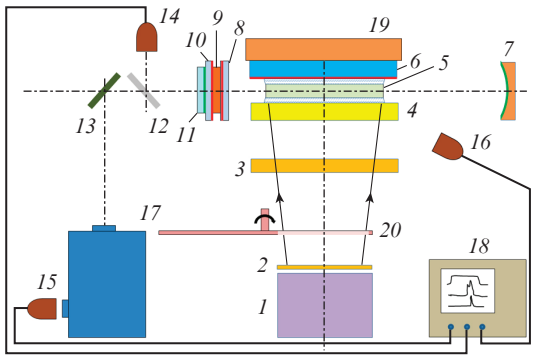

Figure 1. Scheme of the experimental setup: (*1*) laser diode array; (*2*) cylindrical collimating lens; (*3*) focusing cylindrical lens; (*4*) MgF_2 plate; (*5*) Er:YLF crystal; (*6*) gold mirror on a sapphire plate; (*7*) aluminium spherical mirror; (*8*) and (*10*) dichroic mirrors with large reflection coefficients at $\lambda = 4–4.5$ μm and large transmission coefficients at $\lambda = 2.6–2.8$ μm; (*9*) Fe:ZnSe crystal; (*11*) dichroic mirror with a high reflection coefficient in a vicinity of $\lambda = 2.7$ μm and transmitting in the vicinity of 4.2 μm with $T \approx 65\%$; (*12*) removable folding mirror; (*13*) folding mirror; (*14*), (*15*), and (*16*) photodiodes; (*17*) monochromator; (*18*) oscilloscope; (*19*) copper heat sink cooled by water; (*20*) mechanical interrupter.

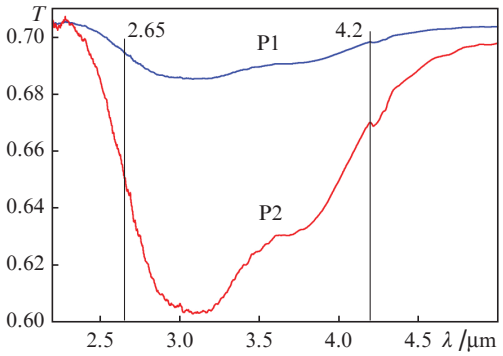

Figure 2. Transmission spectra of Fe:ZnSe plates. The vertical straight lines indicate the wavelengths of laser generation on Er:YLF (2.65 μm) and Fe:ZnSe (4.2 μm) crystals.

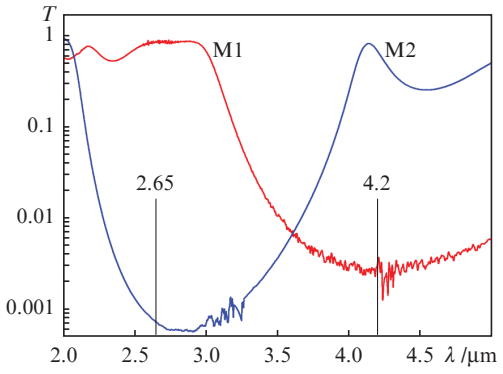

Figure 3. Transmission spectra of mirrors M1 and M2 used as mirrors (*8*), (*10*), and (*11*) (see Fig. 1), respectively.

Preliminary characteristics of the laser based on the assembly of crystal (*9*) and mirrors (*8*) and (*10*) were investigated by pumping by giant pulses from the Er:YAG laser with a *Q*-switched resonator, whose scheme is presented in work [9]. The maximum pump pulse energy was 25 mJ for a pulse duration of 40 ns. The beam diameter in the assembly was 2 mm. Pump radiation and laser radiation were recorded with a FSG-22 photoresistors based on germanium doped with gold and cooled by liquid nitrogen. The time resolution was ~ 5 ns. In these preliminary experiments, we studied the possibility of attaining lasing in the Fe:ZnSe laser using a miniresonator at room temperature, and estimated the threshold pump pulse energy. The pulse energy was varied by means of calibrated filters.

The Er:YLF crystal with the Er concentration of 15% had a length of 28 mm, a width of 4 mm, and a thickness of 2 mm. The polished end faces of 4×2 mm in size were coated with an antireflection coating corresponding to a generation wavelength of about 2.7 μm with a residual reflection coefficient of less than 0.5%. Two lateral surfaces, each of 28×2 mm in size, were coated with an antireflection coating for a pump radiation wavelength of 975 nm with a residual reflection coefficient of less than 0.5%. The faces of 28×4 mm in size were matte. Initially, this crystal was pumped through a lateral surface of 28×2 mm in size. However, in order to reduce the excitation region volume and the generation threshold, it was decided to perform the pumping through the faces of 28×4 mm in size. Crystal (*5*) (see Fig. 1) was attached with the EPOTEK-301 epoxy glue to the sapphire plate (*6*) with a layer of gold deposited on it. A gold layer with a high reflection coefficient in the IR region returned the pump radiation, which was unabsorbed in one pass of the crystal, back to the absorption region. Close values of the refractive indices of the glue ($n_g = 1.52$) and Er:YLF crystal ($n_{YLF} = 1.45$) provided a weak scattering of pump radiation at the glue–crystal interface. To reduce the pump radiation scattering on the input face, a MgF_2 plate (*4*) with a refractive index of $n_{MgF_2} = 1.37$ was also glued to the crystal. The sapphire plate was attached to a copper cold conductor (*19*) cooled by running water. The Er:YLF-laser resonator was formed by a spherical Al-coated mirror (*7*) having a curvature radius of 100 mm, and by a plane mirror (*11*) (transmission spectrum of M2 in Fig. 3). The resonator physical length was 100 mm, i. e. the resonator was close to a semiconcentric one.

The Er:YLF crystal was pumped along the normal to the resonator optical axis by radiation from the array (*1*) of laser diodes mounted on a copper heat sink cooled by running water. The radiation from the laser diode array was collimated by a cylindrical lens (*2*) and focused on the Er:YLF crystal face by a focusing cylindrical lens with a focal length $F = 30$ mm. The radiating surface of the laser diode array was located at a distance of 240 mm from the Er:YLF crystal face, which provided the crystal illumination along the entire length, though the pump radiation intensity of the crystal central part was significantly higher than the pump intensity near the crystal end faces. The crystal was pumped along a strip with a width of ~ 50 μm and a length of 28 mm. The pumped region depth corresponded to the crystal thickness of 2 mm. A maximum output power of the laser diode array was 50 W. In order to reduce the crystal Er:YLF heating, the pump radiation was interrupted by a mechanical interrupter (*20*) made in the form of a rotating disk with slots. The pulse duty cycle was 12.5. The wavelength at the maximum of the pump radiation spectrum varied from 975 to 980 nm with increasing pump power to the maximum value. In this case, the absorption coefficient of the Er:YLF crystal changed slightly. The fraction of the pump power absorbed in the crystal is estimated at 50%.

The oscillograms of the pump and generation pulses were recorded using PD-36 and PD-48 photodiodes (IBSG Co., Ltd). The first type photodiode has a higher sensitivity, which, however, drops sharply at $\lambda > 3.6$ μm. The peak of PD-48 sensitivity is close to $\lambda = 4.5$ μm. Three types of photodiodes were used in the measurements: (*14*), (*15*), and (*16*). Photodiode (*14*) recorded the spectrum-integrated laser pulse, photodiode (*15*) recorded the generation pulse at a certain wavelength cut out by a monochromator (*17*) (MDR-4 with a grating ruled at 150 lines mm^{-1}), and photodiode (*16*) recorded the scattered radiation of the pump pulse. The signals from the photodiodes were directed to an oscilloscope (*18*) (Tektronics TDS 2024B). The resistance of the photodiode load varied from 50 Ω (which provided a better temporal resolution) to 51 kΩ (which provided an increase in the signal when recording the laser pulse passed through the monochromator).

3. Experimental results and their discussion

3.1. Fe:ZnSe laser pumped by giant pulses of Er:YAG laser

Figure 4a shows the oscillograms of pump and generation pulses in the Fe:ZnSe (P2) crystal in a miniresonator formed by mirrors M1. It can be seen that the generation pulse with a moderate threshold excess arises by the end of the pump pulse and has relaxation oscillations. As the excitation energy increases, the start of the generation pulse shifts to the start of the pump pulse, and the pulse energy increases. These changes are typical for the pulsed regime. The threshold pump energy is estimated to be 1 mJ. We should note that the absorbed pump energy is much smaller. The fraction of the pump energy absorbed in the Fe:ZnSe crystal does not exceed ~8% if the absorption saturation is not taken into account. Thus, the threshold absorbed pump energy constitutes ~100 μJ.

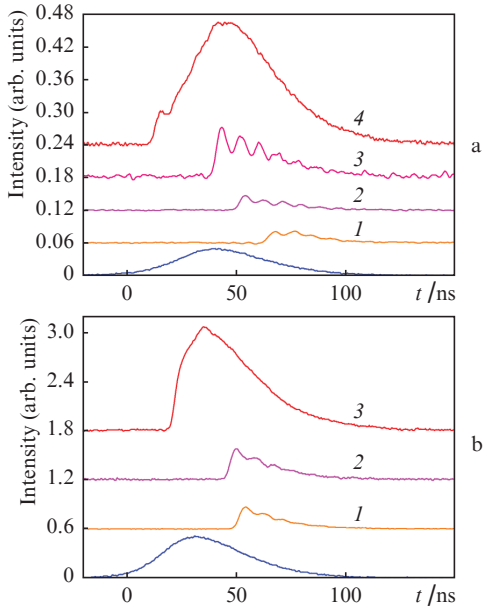

Figure 4. Oscillograms of the pump pulses (bottom curves) and of the generation pulses in the Fe:ZnSe crystal using different filters attenuating the pump energy and output mirrors (a) with $R_{out} = 99.36\%$ at excitation energies E/E_p = (*1*) 0.0558, (*2*) 0.072, (*3*) 0.208, and (*4*) 1.0 and (b) 97.5% at E/E_p = (*1*) 0.159, (*2*) 0.208, and (*3*) 1.0. The pump energy is 25 mJ, the resonator length is 1.7 mm, and $R_1 = 99.36\%$.

Figure 4b shows similar oscillograms, but using a different output mirror with a calculated reflectance of 97.5% for the radiation incident from ZnSe ($n_{ZnSe} = 2.4$). In this case, the laser pulse energy was increased by about four times, and the threshold energy of the pump pulse – to about 3 mJ.

3.2. Er:YLF laser

First, we investigated the Er:YLF laser without assembling elements (*8*), (*9*), and (*10*). As an output mirror (*11*), we used a highly reflecting mirror M2 with a transmittance less than 0.1% at wavelengths near 2.7 μm. Figure 5 shows the oscillograms of the pump pulse and the laser pulses that are spectrum-integrated and passed through a monochromator tuned to wavelengths of 2.65 and 2.71 μm. The pump pulse duration was 5.5 ms.

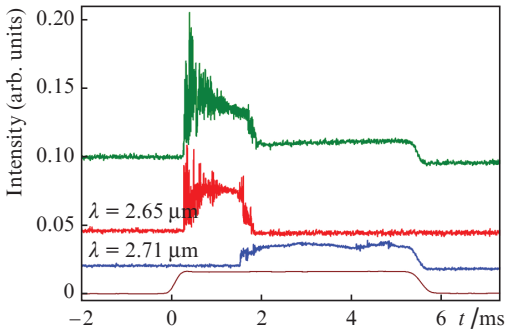

Figure 5. Oscillograms of the pump pulse (bottom curve) and the pulses of Er:YLF laser radiation integrated over spectrum (top curve), and also at wavelengths of 2.65 and 2.71 μm. The radiation was recorded by a PD-36 photodiode. The pump radiation power was 50 W. Passive *Q*-switch was absent.

The generation start corresponds to $\lambda = 2.65$ μm. The generation threshold is ~4 W. Then, the generation proceeds to $\lambda = 2.71$ μm. The time moment of this transition is shifted toward the pump pulse start as the pump power increases, i.e. the generation at $\lambda = 2.71$ μm is more high-threshold. This generation type is typical for the Er:YLF laser [13, 17]. Moreover, when pumping by cw radiation, the generation passes to $\lambda \approx 2.81$ μm [11], but this requires greater pump powers.

The average laser radiation power using a highly reflecting resonator was predictably low and did not exceed 1 mW at a duty cycle of 12.5. The power was measured by a Gentec TPM-300 power meter with a PS-310 measuring head. When the highly reflecting output mirror was replaced by a mirror with a transmittance of 9%, the power increased significantly and amounted to ~45 mW. The average pulse power in this case was 0.56 W with an input pump power of ~25 W. The laser efficiency obtained (~2.2%) was significantly less than the efficiency of 15% attained in [11]. This is primarily due to poor spatial matching of the excitation region with the generated modes of the resonator.

Provided the plate P1 is placed inside the Er:YLF laser resonator as a passive *Q*-switch, short pulses are generated, and the threshold pump power increases up to 17–18 W. Typical oscillograms of the generation pulses are shown in Fig. 6.

In the initial part of the pump pulse, short pulses are generated at $\lambda = 2.65$ μm. Their appearance is chaotic. In the final part of the pump pulse, the laser pulses follow less frequently

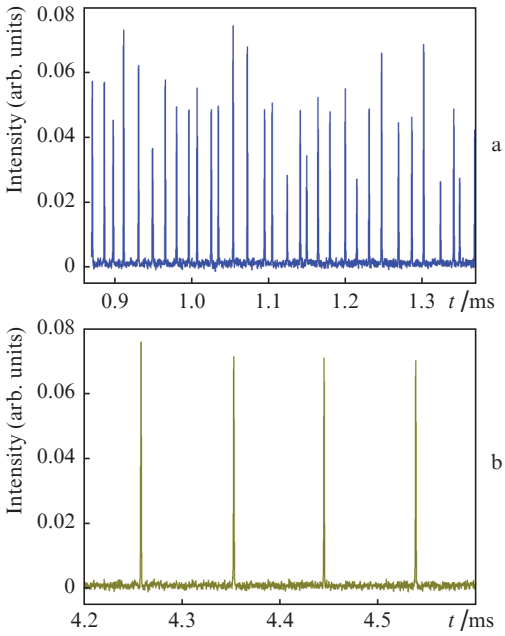

Figure 6. Typical oscillograms of the radiation pulses of the Er:YLF-laser with a passive *Q*-switch (P1), recorded (a) at the pump pulse start ($\lambda = 2.65$ μm) and (b) at the pump pulse end ($\lambda = 2.71$ μm). The pump radiation power is 50 W.

and more regularly. At the same time, their peak power did not increase significantly compared to the peak power of the pulses generated at the pump pulse start. This is due to the fact that the pump power slightly exceeds the threshold power. The duration of laser pulses is ~300 ns in the initial part of the pump pulse, and ~400 ns in its final part.

When the passive *Q*-switch P1 was replaced by the *Q*-switch P2 with a higher absorption coefficient, the generation pulses did not arise in the final part of the pump pulse, since the generation threshold at $\lambda = 2.71$ μm was not reached. The threshold of radiation generation at $\lambda = 2.65$ μm increased to 25 W. The oscillograms of the pump and generation pulses obtained using the *Q*-switch P2 are shown in Fig. 7. The duration of the laser pulses was 130–150 ns.

Since giant pulses only appeared in the front part of the pump pulse with duration of ~5.5 ms, we used pump pulses with a duration of 0.5–1 ms.

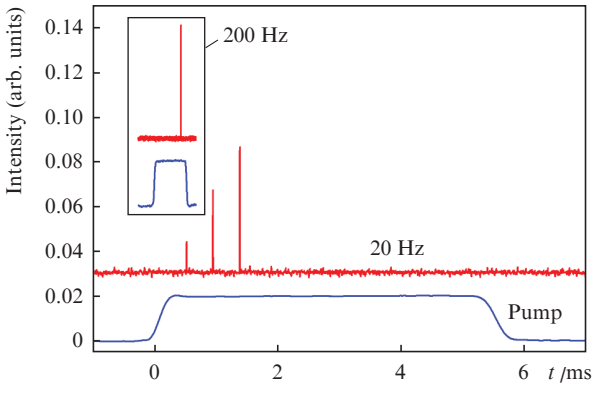

Figure 7. Oscillograms of the generation and pump pulses with repetition rates of 20 and 200 Hz. The pump radiation power is 50 W.

3.3. Fe:ZnSe laser pumped inside the Er:YLF laser resonator

When the assembly of elements (*8*), (*9*) and (*10*) was olaced inside the Er:YLF laser resonator , the shape of the giant pulses changed significantly. Typical oscillograms of individual giant pulses are shown in Fig. 8.

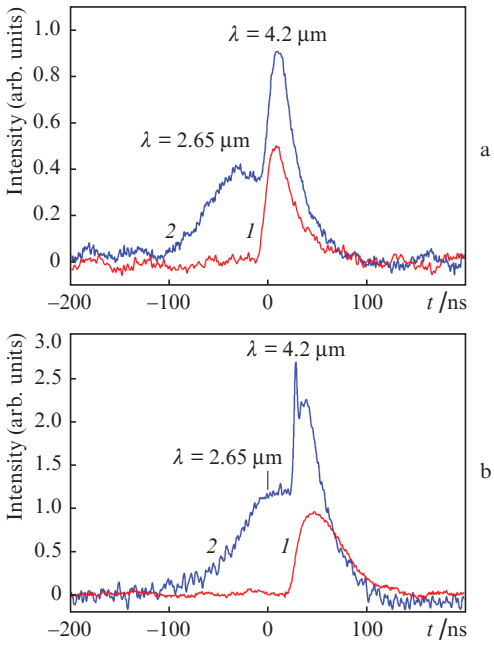

Figure 8. Oscillograms of Er:YLF laser pulses with a passive *Q*-switch (P2) having its own miniresonator: (a) radiation was recorded by a PD-48 photodiode (*1*) after passing through the filter (mirror M2) and (*2*) in its absence; (b) comparison of the oscillograms recorded (*2*) before passing through the monochromator and (*1*) after passing through the monochromator tuned to a wavelength of 4.2 μm. The pump radiation power is 50 W.

The entire giant pulse had a FWHM of about 100 ns (see Fig. 8a). Its shape was determined by the imposition of a short pulse with a FWHM of less than 50 ns onto a longer pulse with a FWHM of 100 ns. If a filter (mirror M2) that cuts off the radiation at $\lambda = 2.65$ μm was placed in front of the recording PD-48 photodiode, only a short pulse remained in the oscillogram. We assumed that this is the generation pulse of the Fe:ZnSe laser, while the wider pulse is the radiation of the Er:YLF laser. To confirm this assumption, the laser pulse was passed through a monochromator. As a result, the radiation pulses were recorded both at a wavelength of 2.65 μm and at a wavelength of 4.2 μm. In using a recording system with a high time resolution in the generation pulse before entering the monochromator, relaxation oscillations were observed in the long-wavelength component (see Fig. 8b). After passing the monochromator, the radiation power was substantially attenuated, and for its reliable recording, a greater load resistance of the photodiode was used, which diminished the temporal resolution.

At a pump pulse repetition rate of 160 Hz, the average laser radiation power was 0.2–0.3 mW. In each pulse, on average, a single giant pulse was generated. Based on this, the energy of the giant pulse can be estimated as 1.5 μJ. The fraction of radiation at $\lambda = 4.2$ μm in this pulse is no less than 30%. Hence, the estimate of the radiation pulse energy of the

Fe:ZnSe laser yields 0.5 μJ. With a pulse duration of 50 ns, this corresponds to a peak power of 10 W.

Let us set the energy of the Er:YLF laser pulse equal to 1 μJ. Given the low transmittance of the output mirror of this laser, the pulse energy inside the resonator can reach 1 mJ. This value is comparable with the obtained estimate for the threshold generation of the Fe:ZnSe laser with external pumping (1 mJ). However, taking into account that the cross-sectional area of the beam inside the resonator (< 0.2 mm^2) is noticeably smaller than the excitation area by external pumping (> 3 mm^2), and the absorption efficiency of pumping by a crystal inside the resonator is significantly higher than in single-pass pumping, we may conclude that a fairly large excess of the generation threshold of the Fe:ZnSe laser with a mini-resonator is attained inside the Er:YLF laser resonator.

The generation spectrum width of Fe:ZnSe laser, measured by a monochromator, was ~ 70 nm. The radiation divergence was estimated by means of the signal change using PD-48 when it was scanned in the focal plane of the CaF_2 lens with a focal length of 89 mm. The total divergence angle constituted ~ 15 mrad. This is approximately twice as large as the divergence angle of the Er:YLF laser radiation. The radiation directivity of the Fe:ZnSe laser can be improved by increasing the transmission of mirror (*8*) and using a composite resonator with a spherical mirror (*7*) (see Fig. 1).

4. Conclusions

We have proposed a new scheme for the Fe:ZnSe laser that generates nanosecond pulses at room temperature of the active crystal. The crystal is pumped inside the Er:YLF laser resonator, in which the active element is in turn pumped by radiation from the laser diode array along the normal to the resonator axis. Pumping is performed in the pulse-periodic regime with a repetition rate of 20–200 Hz and a duty cycle of 12.5. The active element of the Fe:ZnSe laser simultaneously serves as a passive *Q*-switch for the Er:YLF laser. At the output of the Er:YLF laser, giant pulses of 50–100 ns duration are recorded, which represent a superposition of two generation pulses at wavelengths of 2.65 and 4.2 μm. The second pulse is shifted relative to the first one by 20–40 ns. The energies of these pulses are estimated as 1 and 0.5 μJ, respectively. The first pulse represents radiation from the Er:YLF laser, while the second pulse – from the Fe:ZnSe laser. Further research is needed to increase the pulse energy, average power, and efficiency of the Fe:ZnSe laser.

Acknowledgements. The work was supported by the Presidium of the Russian Academy of Sciences (Actual Problems of Photonics, Probing of Inhomogeneous Media and Materials Programme No. 7) and, in part, by the Programme of Increasing the Competitiveness of the National Research Nuclear University 'MEPhI' (Project No. 02.a03.21.0005).

References

1. Adams J.J., Bibeau C., Page R.H., Krol D.M., Furu L.H., Payne S.A. *Opt. Lett.*, **24**, 1720 (1999).
2. Akimov V.A., Voronov A.A., Kozlovskii V.I., Korostelin Yu.V., Landman A.I., Podmar'kov Yu.P., Frolov M.P. *Quantum Electron.*, **34**, 912 (2004) [*Kvantovaya Elektron.*, **34**, 912 (2004)].
3. Fedorov V.V., Mirov S.B., Gallian A., Badikov V.V., Frolov M.P., Korostelin Yu.V., Kozlovsky V.I., Landman A.I., Podmar'kov Yu.P., Akimov V.A., Voronov A.A. *IEEE J. Quantum Electron.*, **42**, 907 (2006).
4. Kozlovsky V.I., Korostelin Y.V., Podmar'kov Y.P., Skasyrsky Y.K., Frolov M.P. *J. Phys.: Conf. Ser.*, **740**, 012006 (2016).
5. Vasilyev S., Moskalev I., Mirov M., Smolski V., Martyshkin D., Fedorov V., Mirov S., Gapontsev V. *Proc. SPIE*, **10193**, 101930U (2017).
6. Frolov M.P., Korostelin Yu.V., Kozlovsky V.I., Podmar'kov Yu.P., Skasyrsky Ya.K. *Opt. Lett.*, **43**, 623 (2018).
7. Firsov K.N., Frolov M.P., Gavrishchuk E.M., Kazantsev S.Yu., Kononov I.G., Korostelin Yu.V., Maneshkin A.A., Velikanov S.D., Yutkin I.M., Zaretsky N.A., Zotov E.A. *Laser Phys. Lett.*, **13**, 015002 (2016).
8. Velikanov S.D., Zaretskiy N.A., Zotov E.A., Kozlovsky V.I., Korostelin Yu.V., Krokhin O.N., Maneshkin A.A., Podmar'kov Yu.P., Savinova S.A., Skasyrsky Ya.K., Frolov M.P., Chuvatkin R.S., Yutkin I.M. *Quantum Electron.*, **45**, 1 (2015) [*Kvantovaya Elektron.*, **45**, 1 (2015)].
9. Akimov V.A., Voronov A.A., Kozlovskii V.I., Korostelin Yu.V., Landman A.I., Podmar'kov Yu.P., Frolov M.P. *Quantum Electron.*, **36**, 299 (2006) [*Kvantovaya Elektron.*, **36**, 299 (2006)].
10. Voronov A.A., Kozlovsky V.I., Korostelin Yu.V., Landman A.I., Podmar'kov Yu.P., Polushkin V.G., Ragimov T.I., Skasyrsky Ya.K., Filipchuk M.Yu., Frolov M.P. *Bull. Lebedev Phys. Inst.*, **37** (6), 169 (2010) [*Kr. Soobshch. Fiz. FIAN*, **37**, 9 (2010)].
11. Dergachev A., Flint J.H., Isyanova Y., Pati B., Slobodtchikov E.V., Wall K.F., Moulton P.F. *IEEE J. Sel. Top. Quantum Electron.*, **13**, 647 (2007).
12. Messner M., Heinrich A., Unterrainer K. *Appl. Opt.*, **57**, 1497 (2018).
13. Inochkin M.V., Nazarov V.V., Sachkov D.Yu., Khloponin L.V., Khramov V.Yu., Korostelin Yu.V., Landman A.I., Podmar'kov Yu.P., Frolov M.P. *Opt. Zh.*, **79**, 31 (2012).
14. Basiev T.T., Denker B.I., Mirov S.B., Osiko V.V., Park V.G., Prokhorov A.M., Kertesz I., Kroo N., Ferencz K. *OSA TOPS Adv. Sol. St. Lasers*, **5**, 332 (1989).
15. De Rossi W., Costa F.E., Vieira N.D. Jr., Wetter N.U., Morato S.P., Basiev T.T., Konyushkin V.A., Mirov S.B. *Appl. Opt.*, **31**, 2719 (1992).
16. Kozlovsky V.I., Akimov V.A., Frolov M.P., Korostelin Yu.V., Landman A.I., Martovitsky V.P., Mislavskii V.V., Podmar'kov Yu.P., Skasyrsky Ya.K., Voronov A.A. *Phys. Stat. Sol. B*, **247**, 1553 (2010).
17. Inochkin M.V., Nazarov V.V., Sachkov D.Yu., Khloponin L.V., Khramov V.Yu. *J. Opt. Technol.*, **77**, 413 (2010).